Structure of the SO_2F^- Anion, a Problem Case[1]

Enno Lork,[†] Rüdiger Mews,*[,†] Detlef Viets,[†] Paul G. Watson,[†] Tobias Borrmann,[†] Ashwani Vij,[‡] Jerry A. Boatz,[‡] and Karl O. Christe*[,‡,§]

Department of Chemistry, University of Bremen, Leobener Strasse NW2, P.O. Box 330440, D-28334 Bremen, Germany, Air Force Research Laboratory, Edwards Air Force Base, California 93524, and Loker Hydrocarbon Research Institute, University of Southern California, Los Angeles, California 90089-1661

Received June 6, 2000

Recently, room-temperature crystal structures of SO_2F^- in its K^+ and Rb^+ salts were published in *Z. Anorg. Allg. Chem.* **1999**, *625*, 385 and claimed to represent the first reliable geometries for SO_2F^-. However, their almost identical S−O and S−F bond lengths and O−S−O and O−S−F bond angles are in sharp contrast to the results from theoretical calculations. To clarify this discrepancy, the new $[(CH_3)_2N]_3SO^+$ and the known $[N(CH_3)_4^+]$, $[(CH_3)_2N]_3S^+$, and K^+ salts of SO_2F^- were prepared and their crystal structures studied at low temperatures. Furthermore, the results from previous RHF and MP2 calculations were confirmed at the RHF, B3LYP, and CCSD(T) levels of theory using different basis sets. It is shown that all the SO_2F^- salts studied so far exhibit varying degrees of oxygen/fluorine and, in some cases, oxygen-site disorders, with $[(CH_3)_2N]_3SO^+SO_2F^-$ at 113 K showing the least disorder with r(S−F) − r(S−O) = 17 pm and ∠(O−S−O) − ∠(F−S−O) = 6°. Refinement of the disorder occupancy factors and extrapolation of the observed bond distances for zero disorder resulted in a geometry very close to that predicted by theory. The correctness of the theoretical predictions for SO_2F^- is further supported by the good agreement between the calculated and the experimentally observed vibrational frequencies and their comparison with those of isoelectronic ClO_2F. A normal coordinate analysis of SO_2F^- confirms the weakness of the S−F bond with a stretching force constant of only 1.63 mdyn/Å and shows that there is no highly characteristic S−F stretching mode. The S−F stretch strongly couples with the SO_2 deformation modes and is concentrated in the two lowest a′ frequencies.

Introduction

The SO_2F^- anion has been known since 1953 from the work of Seel and co-workers.[2−5] Its vibrational spectra were studied by Seel and Boudier,[6] Paetzold and Aurich,[7] Robinson and co-workers,[8] Moock and co-workers,[9] and Kornath and co-workers[10] and correctly assigned with the help of ab initio calculations in terms of a C_s symmetry structure with a predicted geometry of r(S−F) = 170 pm, r(S−O) = 146 pm, ∠(O−S−O) = 113.2°, and ∠(O−S−F) = 100.6°.[10] The agreement between observed and calculated vibrational frequencies was good and supported the calculated geometry. Furthermore, the calculated geometry of SO_2F^- is similar to that experimentally observed for isoelectronic ClO_2F.[11]

The geometry predicted from the theoretical calculation and supported by the vibrational analysis[10] is in conflict with the results from three recent X-ray diffraction studies. Zhu and co-workers reported the crystal structure of $Ph_3PCF_2H^+SO_2F^-$.[12] In this structure, the SO_2F^- anion is both fluorine/oxygen and oxygen-site disordered, and its geometry was listed as r(S−F) = 151.6(6) pm, r(S−O(1)) = 143.6 pm, r(S−O(2)) = 141(1) pm, and ∠(F−S−O(1)) = 110.5(5)°. The second structure was obtained by Kuhn and co-workers for 2-fluoro-1,3-diisopropyl-4,5-dimethylimidazolium fluorosulfite.[13,14] In this structure, the SO_2F^- anion is similarly disordered, and therefore, the authors considered a discussion of the SO_2F^- geometry inappropiate.[13] In the most recent study by Kessler and Jansen,[15] the room-temperature structures of KSO_2F and $RbSO_2F$ were given with r(S−F) = 159.1(2) pm, r(S−O) = 152.6(2) pm, ∠(O−S−O) = 104.9(2)°, and ∠(O−S−F) = 102.8(1)° for the K^+ salt. Possible disorder was ignored, and the obtained structural parameters were taken as the correct geometry of isolated SO_2F^-, concluding that the previously published,[10,14] theoretically calculated structures were invalid. This conclusion, however, raises serious questions. Above all, how could a geometry which deviates by 18 pm for r(S−F) and by 8° for ∠(O−S−O) from the true structure duplicate well the observed vibrational frequencies?

In this paper we report the preparation of the $(Me_2N)_3S^+$ (TAS),[16] $(Me_2N)_3SO^+$ (TAOS), $N(CH_3)_4^+$ (TMA),[3,4] and K^+

[†] University of Bremen.
[‡] Air Force Research Laboratory.
[§] University of Southern California.

(1) Experimental results from this study and preliminary conclusions were reported by E. Lork, T., Borrmann, D. Viets, W.-D. Stohrer, and R. Mews at the 12th European Symposium on Fluorine Chemistry, Berlin, Germany, August 1998, paper B33.
(2) Seel, F.; Meier, H. *Z. Anorg. Allg. Chem.* **1953**, *274*, 202.
(3) Seel, F.; Jonas, H.; Riehl, L.; Langer J. *Angew. Chem.* **1955**, *67*, 32.
(4) Seel, F.; Riehl, L. *Z. Anorg. Allg. Chem.* **1955**, *282*, 293.
(5) Seel, F.; Gölitz, D. *Z. Anorg. Allg. Chem.* **1964**, *327*, 28.
(6) Seel, F.; Boudier, J. *Z. Anorg. Allg. Chem.* **1966**, *342*, 173.
(7) Paetzold, R.; Aurich, K. *Z. Anorg. Allg. Chem*. **1965**, *335*, 281.
(8) Robinson, E. A.; Lavery, D. S.; Weller, S. *Spectrochim. Acta* **1968**, *25A*, 151.
(9) Moock, K. H.; Sülzle, D.; Klaboe, P. *J. Fluorine Chem.* **1999**, *47*, 151.
(10) Kornath, A.; Neumann, F.; Ludwig, R. *Inorg. Chem.* **1997**, *36*, 5570.
(11) Robiette, A. G.; Parent, C. R.; Gerry, M. C. L. *J. Mol. Struct.* **1981**, *86*, 455.
(12) Zhu, S. Z.; Huang, Q.-C.; Wu, K. *Inorg. Chem.* **1994**, *33*, 4585.
(13) Kuhn, N.; Bohnen, H.; Fahl, J.; Boese, R. *Chem. Ber.* **1996**, *129*, 1579.
(14) Maulitz, A. H.; Boese, R.; Kuhn, N. J. *J. Mol. Struct*. **1995**, *333*, 227.
(15) Kessler, U.; Jansen, M. *Z. Anorg. Allg. Chem.* **1999**, *625*, 385.
(16) Heilemann, W.; Mews, R. *Chem. Ber*. **1988**, *121*, 461.

10.1021/ic000616p CCC: $20.00
Published on Web 02/16/2001

salts of SO_2F^- and their low-temperature crystal structures. It is shown that the true geometry of SO_2F^- is close to the calculated ones and that the varying degrees of deviation, exhibited in the crystal structures of the different salts, are due to the propensity of SO_2F^- to undergo oxygen/fluorine and, in some cases, oxygen-site disorders.

Experimental Section

Standard inert atmosphere techniques were used for the manipulation of all reagents and reaction products. Infrared spectra were recorded on a Nicolet DX-55-FT-IR spectrometer using Nujol/Kel-F mulls, and NMR spectra on a Bruker WP80SY referenced to Me_4Si (^1H) and $CFCl_3$ (^{19}F). The NMR samples, dissolved in liquid SO_2, were contained in sealed 5 mm glass tubes. Commercial grade solvents (MeCN, Et_2O) were dried and purified by employing conventional procedures.[17] Commercial SO_2 was stored over P_4O_{10} at room temperature. TAOSF was obtained, similarly to TASF, from OSF_4 and Me_3SiNMe_2;[18] TASF[16,19] and TMAF[20] were prepared as described, and the fluorosulfites were synthesized according to the method reported for $TAS^+SO_2F^-$.[16] The spectroscopic data of $TAS^+SO_2F^-$ (**1**) and $TMA^+SO_2F^-$ (**3**) agreed with those reported in the literature.[3,4,16]

$TAOS^+SO_2F^-$ **(2)** was obtained by dissolving $TAOS^+Me_3SiF_2^-$ (1.7 mmol) in 10 mL of SO_2 at −30 °C. The solution was stirred for 30 min at this temperature, and then all volatile material was removed under vacuum. **2** (0.45 g, 100% yield) remained as a colorless solid, mp 239 °C dec.

Salts **1**−**3** were recrystallized from MeCN/Et_2O mixtures at −40 °C to give single crystals suitable for X-ray structure determinations.

Crystal Structure Determinations. The crystals were mounted onto thin glass fibers using the oil-drop technique (Kel-F oil). The data were collected on a Siemens P4 diffractometer using Mo Kα radiation (λ = 71.073 pm) at the given temperatures. The structures were solved by direct methods. Hydrogen atoms were located from difference electron density maps and refined isotropically.

Computational Methods. The geometries and harmonic vibrational frequencies of SOF_2, SO_2F_2, and SO_2F^- were calculated using restricted Hartree−Fock (RHF), density functional theory (using the B3LYP hybrid functional[21]), and coupled-cluster (CCSD(T)[22]) methods. The 6-311+G(2d)[23] and the augmented correlation-consistent polarized valence double- and triple-ζ basis sets[24] were used. All calculations were performed using GAMESS[25] and GAUSSIAN 94.[26]

Results and Discussion

Synthesis and Properties of $TAOS^+SO_2F^-$. TAS fluoride, $(Me_2N)_3S^+Me_3SiF_2^-$,[19] is an excellent fluoride ion donor which readily transfers a fluoride ion to the more acidic SO_2 molecule.[16]

$$TAS^+Me_3SiF_2^- + SO_2 \xrightarrow[-30\ °C]{SO_2} TAS^+SO_2F^- + Me_3SiF$$

Replacement of TASF by TAOSF, $(Me_2N)_3SO^+Me_3SiF_2^-$, results in the corresponding $TAOS^+SO_2F^-$ salt in quantitative yield.

$$TAOS^+Me_3SiF_2^- + SO_2 \xrightarrow[-30\ °C]{SO_2} TAOS^+SO_2F^- + Me_3SiF$$

The new $TAOS^+SO_2F^-$ salt is a colorless solid that is stable at room temperature and melts at 239 °C with decomposition. It was characterized by its crystal structure (see below).

Crystal Structures of $TAS^+SO_2F^-$ (1), $TAOS^+SO_2F^-$ (2), $TMA^+SO_2F^-$ (3), and $K^+SO_2F^-$ (4). The crystal structures of **1**−**4** were determined at 173 K and those of **2** and **4** also at 113 K. The crystal and structure refinement data and the bond distances and angles of the SO_2F^- anions are given in Tables 1 and 2, respectively. The molecular units with atom labeling, the packing diagrams, and the closest anion−cation interactions are shown in Figures 1−7. As can be seen, compounds **1**−**4** are predominantly ionic, containing isolated SO_2F^- anions.

The refinement of the $TAS^+SO_2F^-$ (**1**) structure was not trivial. Initial structure refinements in the space group *Pnma* put the atoms S, F, and O(2) on special positions located on a mirror plane, while O(1) was site-disordered, occupying split positions off the plane with occupancy factors of 1/2. In addition, the similarity of the S−O(2) and S−F bond lengths was also indicative of fluorine/oxygen disorder. This solution resulted in an apparent unusually short S−O(1) bond of ∼140 pm, about 5 pm shorter than our theoretical predictions for *r*(S−O), with large thermal motions around the SO(2)F atoms. Since the theoretical calculations also predict that the S−F bonds in SO_2F^- are much longer than the S−O bonds, oxygen/fluorine disorder could only lengthen but not shorten the S−O bonds. The same argument applies to libration corrections. Therefore, this refinement model does not result in a plausible structure for SO_2F^-. The shape of the thermal ellipsoids of the atoms in the SO_2F^- anion suggested that these atoms might be disordered across the crystallographic mirror plane. Furthermore, the analysis of the listing file that was generated by the SHELXTL software suggested that the sulfur and oxygen atoms, S(1) and O(1), could possibly split into two separate positions across the crystallographic mirror plane. After the new coordinates for these two atoms were refined, new q-peaks were found around the sulfur atoms that could be visualized as two SO_2F^- groups disordered across the mirror plane. In accord with the symmetry conditions, the new coordinates of all atoms of one of the two SO_2F^- groups were refined, with the positions of all atoms being forced to be located off this plane by constraining the *y*-coordinates to the values suggested by the SHELXTL program. This procedure resulted in two sets of disordered anions with half-occupancy (see Figure 1). Repeating the refinement without constraining

(17) Perrin, D. D.; Armageo, W. L. F. *Purification of Laboratory Chemicals*, 3rd ed.; Pergamon: London, 1988.
(18) Wessel, J. Dissertation, University of Bremen, Germany, 1995. Wessel, J.; Lork, E.; Behrens, U.; Borrmann, T.; Stohrer, W.-D.; Mews, R. To be published.
(19) Middleton, W. J. U.S. Pat. 3 940 402, 1976; *Org. Synth*. **1985**, *64*, 221.
(20) Christe, K. O.; Wilson, W. W.; Wilson, R. D.; Bau, R.; Feng, J. *J. Am. Chem. Soc.* **1990**, *112*, 7619.
(21) Becke, A. D. *J. Chem. Phys*. **1993**, *98*, 5648.
(22) See, for example: Bartlett, R. J.; Stanton, J. F. Applications of Post-Hartree−Fock Methods: A Tutorial. In *Reviews of Computational Chemistry*; Lipkowitz, A., Boyd, D. B., Eds.; VCH Publishers, Inc.: New York, 1994; Vol. V.
(23) (a) Krishnan, R.; Binkley J. S.; Seeger, R.; Pople J. A. *J. Chem. Phys*. **1980**, *72*, 650. (b) McLean, A. D.; Chandler, G. S. *J. Chem. Phys*. **1980**, *72*, 5639. (c) Frisch, M. J.; Pople, J. A.; Binkley, J. S. *J. Chem. Phys*. **1984**, *80*, 3265. (d) Clark, T.; Chandrasekhan, J.; Spitznagel, G. W.; Schleyer, P. von R. *J. Comput. Chem.* **1983**, *4*, 294.
(24) (a) Dunning, T. H., Jr. *J. Chem. Phys*. **1989**, *90*, 1007. (b) Kendall, R. A.; Dunning, T. H., Jr.; Harrison R. J. *J. Chem. Phys*. **1992**, *96*, 6796. (c) Woon, D. E.; Dunning, T. H., Jr. *J. Chem. Phys*. **1993**, *98*, 1358.
(25) Schmidt, M. W.; Baldridge, K. K.; Boatz, J. A.; Elbert, S. T.; Gordon, M. S.; Jensen, J. J.; Koseki, S.; Matsunaga, N.; Nguyen, K. A.; Su, S.; Windus, T. L.; Dupuis, M.; Montgomery, J. A. *J. Comput. Chem*. **1993**, *14*, 1347.
(26) Frisch, M. J.; Trucks, G. W.; Schlegel, H. B.; Gill, P. M. W.; Johnson, B. G.; Robb, M. A.; Cheeseman, J. R.; Keith, T.; Petersson, G. A.; Montgomery, J. A.; Raghavachari, K.; Al-Laham, M. A.; Zakrzewski, V. G.; Ortiz, J. V.; Foresman, J. B.; Cioslowski, J.; Stefanov, B. B.; Nanayakkara, A.; Challacombe, M.; Peng, C. Y.; Ayala, P. Y.; Chen, W.; Wong, M. W.; Andres, J. L.; Replogle, E. S.; Gomperts, R.; Martin, R. L.; Fox, D. J.; Binkley, J. S.; Defrees, D. J.; Baker, J.; Stewart, J. P.; Head-Gordon, M.; Gonzalez, C.; Pople, J. A. *Gaussian 94*, revision D.4; Gaussian, Inc.: Pittsburgh, PA, 1995.

Table 1. Crystal Data and Structure Refinement for **1**−**4**

	1	**2**	**3**	**4**
empirical formula	$C_6H_{18}FN_3O_2S_2$	$C_6H_{18}FN_3O_3S_2$	$C_4H_{12}FNO_2S$	FKO_2S
mol wt	247.35	263.35	157.21	122.16
T (K)	173(2)	113(2)	173(2)	113(2)
cryst syst	orthorhombic	orthorhombic	orthorhombic	monoclinic
space group	Pnma	$Pna2_1$	Pbca	$P2_1/m$
a (pm)	1469.0(3)	2185.0(2)	1152.0(1)	461.3(1)
b (pm)	1117.4(2)	673.3(1)	1150.5(1)	564.0(1)
c (pm)	733.4(1)	819.4(1)	1162.7(2)	683.0(1)
β (deg)				107.06(1)
V (nm)	1.2038(4)	1.2055(3)	1.5410(3)	0.16988(5)
Z	4	4	8	2
D_c (Mg m^{-3})	1.365	1.451	1.355	2.388
no. of reflns collected	1993	3019	2357	691
no. of independent reflns	1444	2771	1763	427
R(int)	0.0283	0.0810	0.0468	0.0166
no. of params	122	212	135	33
μ(Mo Kα), mm^{-1}	0.438	0.449	0.375	2.000
R1	0.0430	0.0434	0.0517	0.0263
wR2	0.0961	0.1045	0.1275	0.0748
Flack's param		0.01(9)		
difference electron density (e Å^{-3})	0.412/−0.257	0.461/−0.547	0.448/−0.594	0.600/−0.407

Table 2. Bond Distances and Angles of the Fluorosulfite Anion $FSO(1)O(2)^-$ in Different Salts Compared to Those Calculated for the Free Gaseous Anion[a]

compd	r(S−O(1)) (pm)	r(S−O(2)) (pm)	r(S−F) (pm)	∠(O(1)−S−O(2)) (deg)	∠(O(1)−S−F) (deg)	∠(O(2)−S−F) (deg)	temp[b] (K)	ref
1[c]	152.1(3) [O_F = 0.35]	146.2(3) [O_O = 1.0]	155.9(2) [O_O = 0.35]	109.8(2)	108.8(1)	113.0(1)	173	
2	148.3(3) [O_F = 0.19]	146.8(3) [O_O = 1.0]	164.2(2) [O_O = 0.19]	108.8(2)	102.6(2)	102.4(2)	113	
3	151.9(2) [O_F = 0.34]	147.0(2) [O_O = 1.0]	155.6(2) [O_O = 0.34]	106.9(2)	102.7(1)	104.2(1)	173	
4	152.5(2) [O_F = 0.28]	152.5(2)[g] [O_F = 0.28]	162.8(2) [O_O = 0.28]	105.9(1)	101.9(7)	101.9(7)[g]	113	
predicted[h] for free gaseous ion	147	147	170−175	113	100.5	100.5		
KSO_2F (**5**)	152.6(2)	152.6(2)	159.1(2)	104.9(2)	102.8(1)	102.8(1)	294	15[f]
$RbSO_2F$ (**6**)	153.0(6)	153.6(6)	159.8(8)	105.7(5)	102.6(3)	102.6(3)	294	15[f]
$Ph_3PCF_2H^+$[d] (**7**)	143.6()	141.1(1)	151.6(6)		110.5(5)		293	12[f]
F-imid[e] (**8**)	148.9(11)	146.8(14)	149.6(16)	108.7(7)	104.4(8)	107.4(8)	190	13, 14[f]

[a] The data for **5**−**8** are literature values which were not corrected for O/F mixed occupancies and therefore do not represent the true structures. [b] Temperature of data collection. [c] The anion is disordered across a mirror plane. The occupancies of mixed O(1) and F positions (O_O = oxygen occupancy and O_F = fluorine occupancy) are refined. [d] Disordered. [e] F-imid = 2-fluoro-1,3-diisopropyl-4,5-dimethylimidazolium cation. [f] Data uncorrected for mixed O/F occupancies. [g] Symmetry generated: $x, -y + 1/2, z$. [h] Predicted values based on the calculations given in Table 3.

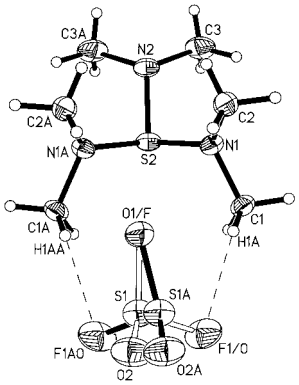

Figure 1. Crystal structure, numbering scheme, and hydrogen bridging of $TAS^+SO_2F^-$ (**1**), showing the two disordered positions of SO_2F^-. The displacement elipsoids are drawn at the 50% probability level, and the hydrogen atoms were located from difference electron density maps.

the y-coordinates resulted in the SO_2F^- anion falling back onto the mirror plane and yielding the previously determined "erroneous" bond distances. Although the refinement with unconstrained SO_2F^- positions results in R values that are reduced by about 0.15%, the resulting geometry is not acceptable. Therefore, our method of refining the disorder offers a better solution to the structural ambiguity and offers a practical approach to visualize the components of the disordered SO_2F^- anion. It also results in a plausible value of 146.5(3) pm for the S−O(2) bond distance, indicating that O(2) is not affected by oxygen/fluorine disorder, and yields a slightly improved R factor.

Since the O(1) and F positions are disordered, the S−O and S−F bond distances and their bond angles could not be uniquely determined in this manner. The disorder was first modeled with equal O(1)/F occupancy factors. However, it was found that the occupancy factors cannot be equal because the two resulting S−O(1)/F bond lengths differed by 3.7 pm. The shortcomings of this model are also apparent from the sum of the O−S−O and O−S−F bond angles, which total 331.6° instead of the theoretically predicted 314°. To obtain the correct occupancy factors which can account for the different S−O(1)/F bond lengths, the sums of the individual occupancy factors were constrained to their required totals (1.0 and 1.0), and the variable individual occupancy factors were refined to give the best fit with the observed data. The occupancy factors of **2**−**4** were refined in the same manner, and the results are summarized in Table 2.

The packing diagram of TAS^+ SO_2F^- (Figure 2) shows a three-dimensional network of intermolecular H···O/F contacts.

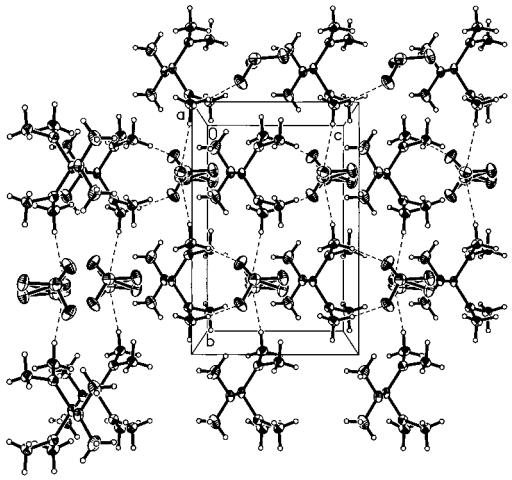

Figure 2. Packing diagram and hydrogen bridging of $TAS^+SO_2F^-$ (**1**).

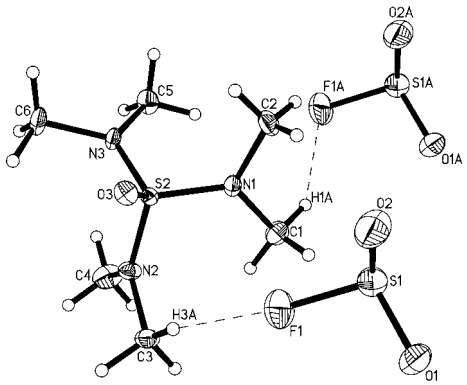

Figure 3. Crystal structure, numbering scheme, and hydrogen bridging of $TAOS^+SO_2F^-$ (**2**) at 113 K. The displacement elipsoids are drawn at the 50% probability level, and the hydrogen atoms were located from difference electron density maps.

Out of the four potential binding sites in the disordered SO_2F^- anion, the F/O atoms form a 10-membered pseudo-ring (Figure 1) with an H(1A)···F/O distance of 250(3) pm. We use the term "pseudo-ring" because one side of the ring structure is always left open due to the disorder-induced half-occupancy. These pseudo-ring structures are then connected to the others in the same plane via the O(2)/O(2A) contacts, i.e., H(1C)···O(2) and H(2C)···O(2) at 258(3) and 266(2) pm, respectively. This network is then linked to the other networks via bonding from O(1)/F(1) at 253(3) pm.

The disorder of the SO_2F^- anion in the TAOS salt is less complicated than that in the TAS salt because it exhibits only the O(1)/F disorder with respect to the mirror plane formed by O(2), S, and the free valence electron pair on sulfur, but not the additional disorder with respect to the crystallographic mirror plane. Furthermore, from all the presently known SO_2F^- structures, that of the TAOS salt at 113 K (Figures 3 and 4) exhibits the least amount of oxygen/fluorine disorder, resulting in the largest differences between the apparent S−F and S−O bond lengths and O−S−O and F−S−O bond angles. The degree of O/F disorder also decreases with decreasing temperature, as was established by carrying out the structure determinations at 173 and 113 K. As in the case of the TAS salt, the S−O(2) bond, which lies on the molecular symmetry plane, is not affected by disorder, resulting in an S−O(2) bond length of 146.8(3) pm, which is, within experimental error, identical to that found for the unique oxygen in the TAS salt and, therefore, should be representative of the true S−O bond length in ordered

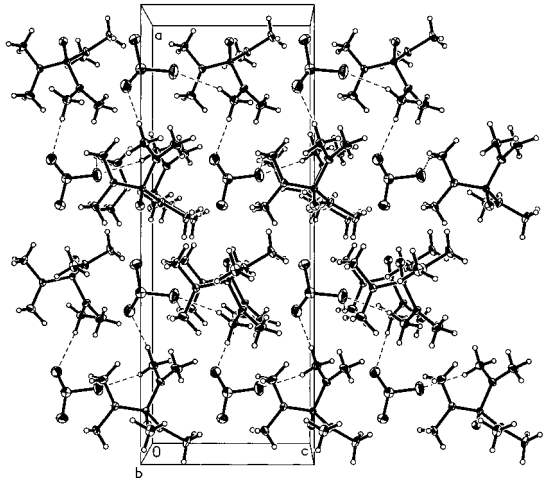

Figure 4. Packing diagram and hydrogen bridging of $TAOS^+SO_2F^-$ (**2**).

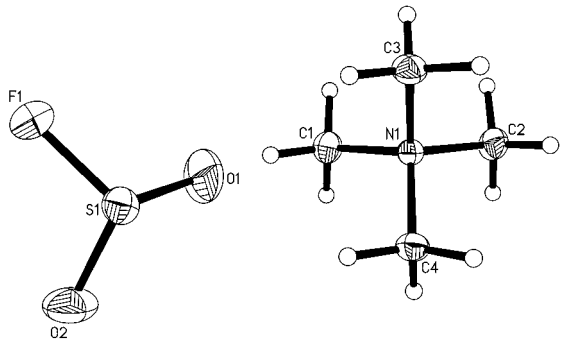

Figure 5. Crystal structure and numbering scheme of $TMA^+SO_2F^-$ (**3**). The displacement elipsoids are drawn at the 50% probability level, and the hydrogen atoms were located from difference electron density maps.

SO_2F^-. Furthermore, the sum of the O−S−O and O−S−F bond angles amounts to 313.9°, which is in excellent agreement with the value of 314° predicted from the ab initio calculations. The facts that r(S−O(1)) and r(S−F) in the 113 K structure of $TAOS^+SO_2F^-$, obtained by refinement assuming an ordered structure, are still somewhat longer and shorter, respectively, than the theoretical predictions for free SO_2F^- and that r(S−O(1)) is 1.6 pm longer than r(S−O(2)) indicate that even in this case there is still some remaining disorder of O(1) and fluorine.

Due to the absence of strong disorder in $TAOS^+SO_2F^-$ at 113 K, its crystal packing (Figure 4) can be discussed more meaningfully. The CH_3 group of C(3) bridges to two SO_2F^- anions via the F(1)···H(3A)−C(3)−H(3C)···O(1) links, forming a zigzag chain (F(1)···H(3A) = 243(3) pm, O(1)···H(3C) = 255(4) pm). These chains then form a three-dimensional network by the formation of an intramolecular bifurcated fluorine contact (H(1A)···F(1) = 246(4) pm). These three contacts are the shortest long-range contact distances[27] in the crystal lattice.

Refinement of the 173 K structure of $TAOS^+SO_2F^-$, assuming no disorder, suffered from shortcomings similar to those previously reported in the literature for the $Ph_3PCF_2H^+$ salt[12] and provided no useful information.

In the $TMA^+SO_2F^-$ salt (see Figures 5 and 6 and Tables 1 and 2) at 173 K, the SO_2F^- anion shows, as in the $TAOS^+$ salt, only O(1)/F disorder with respect to the mirror plane formed by O(2), S, and the free valence electron pair on sulfur, resulting

(27) Bondi, A. *J. Phys. Chem.* **1964**, *68*, 441.

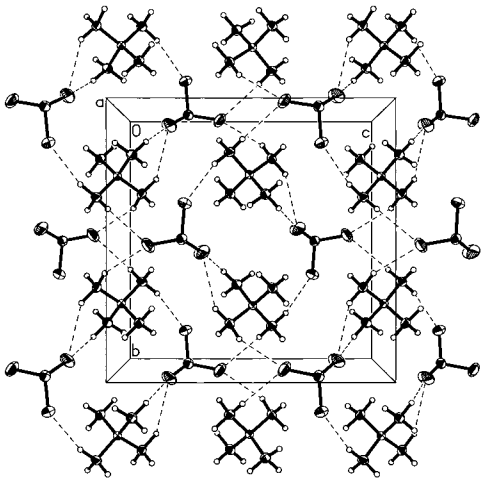

Figure 6. Packing diagram and hydrogen bridging of $TMA^+SO_2F^-$ (**3**).

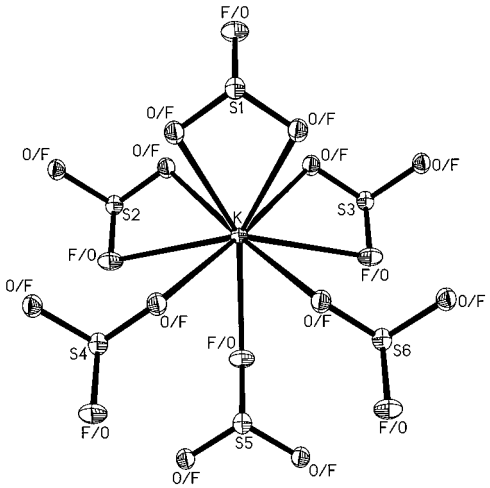

Figure 7. Crystal structure at 113 K and numbering scheme of $K^+SO_2F^-$ (**4**), showing the coordination of six SO_2F^- anions around the K^+ cation.

again in a unique S−O(2) distance of 147.0(2) pm, which is almost identical to those found for the TAS^+ and $TAOS^+$ salts. Refinements, carried out assuming equal occupancy factors for O(1) and F, resulted again in different bond lengths for the two S−O(1)/F bonds, demonstrating the need for refining the occupancy factors.

The packing diagram for $TMA^+SO_2F^-$ is shown in Figure 6 and exhibits bifurcated bridges between O(2) and two hydrogen atoms from the same TMA cation, and between one of the O(1)/F atoms and hydrogen atoms from two different TMA cations, with the other O(1)/F atom forming a single bridge to a TMA cation. The bifurcated bridging is similar to that observed for $TAOS^+SO_2F^-$, resulting in 16-membered rings that contain two cations and two anions and are three-dimensionally cross-linked to other rings. The two shortest of the many close distances are H(2C)···O(1)/F(1) at 235(2) pm and H(1B)···O(2) at 243(2) pm.

The low-temperature (113 K) structure of $K^+SO_2F^-$ is shown in Figure 7. This structure also exhibits oxygen/fluorine disorder, but contrary to the TAS, TAOS, and TMA salt structures, both oxygen atoms participate in the disorder. Therefore, this structure does not provide a unique S−O bond distance. The differences between the KSO_2F and the TAS, TAOS, and TMA salt structures suggest a different kind of disorder. In the TAS, TAOS, and TMA salts, which exhibit significant anion−cation

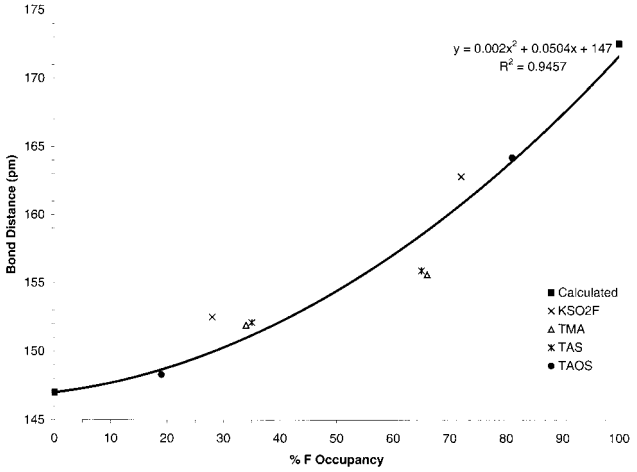

Figure 8. Observed S−O/F and S−F/O bond lengths of **1**−**4** (pm) as a function of their O/F occupancy factors.

interactions through hydrogen bridges, the disorder is related to a symmetry plane through O(2), S, and the free valence electron pair on sulfur, while in the K^+ salt, which exhibits weaker anion−cation bridging, it appears to involve positional disorder around a pseudo-3-fold axis along sulfur and its free valence electron pair. In the positionally disordered structure of KSO_2F, the occupancy factors for the three O/F positions are not equal and one bond is considerably longer than the other two, requiring again a refinement of the occupancy factors. Except for the expected temperature effects, our low-temperature structure of $K^+SO_2F^-$ is essentially identical to that previously found at room temperature,[15] although the longer S−F/O bond is about 4 pm longer at the lower temperature, indicating a decrease in disorder with decreasing temperature.

As can be seen in Figure 7, the potassium ion is surrounded by six SO_2F^- anions. Out of these, three form bidentate and three form monodentate bridges to K^+. Out of the three bidentate SO_2F^- groups, one is bridged through the two atoms with the higher oxygen occupancy factors, designated as O/F; the other two are bridged through one atom with the higher oxygen occupancy factor (O/F) and one atom with the higher fluorine occupancy factor, designated as F/O. Out of the three monodentate SO_2F^- groups, two are bridged through O/F atoms and one through F/O atoms, resulting in an unusual coordination number of 9 around K^+.

The above structure analyses resulted for the TAS, TAOS, and TMA salts in a well-defined S−O(2) distance of about 147 pm that is in excellent agreement with the theoretical predictions (see below). However, in all these structures, the observed S−F distances are too short due to O(1)/F disorder with varying occupancy factors. Since the observed bond lengths should be a function of the corresponding occupancy factors, one should be able to extrapolate to a 100% occupancy factor and thus obtain an estimate for the individual S−F bond length in SO_2F^-. This was done in Figure 8, which shows that the length of the S−F bond should exceed 170 pm, in agreement with the theoretical predictions. The previous conclusion[15] that the geometry derived from the strongly disordered room-temperature structure of KSO_2F represents the first reliable geometry for SO_2F^- is obviously flawed. The pronounced tendency of SO_2F^- to undergo disorder can be attributed to its pyramidal shape, the similar sizes and electronegativities of its ligands, and packing arrangements that favor disorder.

Computational Results. Molecular vibrations occur on a very fast time scale and, therefore, are not affected by disorder

phenomena in the crystal. Furthermore, the vibrational frequencies of a molecule are uniquely determined by its geometry. Therefore, good agreement between observed and calculated frequencies can be obtained only with the correct geometry,[22] and not, as previously implied,[15] with an incorrect geometry. Good-quality theoretical calculations generally yield relatively accurate bond angles.[22] Depending on the level of theory and the quality of the basis set used, the bond distances are generally also accurate within a few picometers. When calculated and observed frequencies are compared, it should be kept in mind that the calculated values are harmonic frequencies while the observed ones are anharmonic, thus giving rise to small discrepancies. Furthermore, different physical states can cause minor deviations. The calculated values are for the isolated free species in the gas phase, while observed spectra are frequently for solids or liquids. However, these effects are generally small, and systematic over- or underestimation of bond lengths and vibrational frequencies at certain levels of theory can be corrected by using scaling factors.

Reliable experimental vibrational spectra for SO_2F^- have recently been published by Kornath and co-workers and were shown to be in reasonable agreement with the values calculated at the uncorrelated RHF/6-31 +G* level of theory.[10] The calculated geometry was also in good agreement with values[14] previously obtained at the RHF/6-31+G(3df) and MP2/6-31+G-(3df) levels of theory. We have calculated the geometry and vibrational frequencies of SO_2F^- at the uncorrelated RHF, the correlated CCSD(T), and the density functional B3LYP levels of theory using 6-311+G(2d),[21] aug-cc-pvdz, and aug-cc-pvtz[22] basis sets. To judge the reliability of these calculations, the geometries and vibrational frequencies of the closely related and well-known SOF_2[28,29] and SO_2F_2[30,31] molecules were also calculated.

The results from these calculations are summarized in Tables 3 and 4, respectively, and show that the bond angles of free SO_2F^- change only little with the method of calculation and the basis set. Values of $\angle$(F−S−O) = 100.5° and $\angle$(O−S−O) = 113° should be close to the actual values. The calculated S−O bond length range in SO_2F^- is also narrow, and this bond is predicted to be about 147 pm, which is in excellent agreement with the value of 146.8(3) pm observed in one of our crystal structure studies. The S−F bond length, however, is more sensitive to the level of theory and quality of the basis set chosen and is predicted to fall into the range of 170−176 pm, which is not too different from the minimum bond length of 165.7 pm derived from our crystal structure studies. This relatively wide range is not surprising since the S−F bond in SO_2F^- is highly polar (see the Normal Coordinate Analysis), and the calculations for highly polar bonds are very sensitive to correlation and basis set polarization functions. On the basis of our predictions (see Table 3), the difference between r(S−F) and r(S−O) should range from 23 to 29 pm, which is in marked contrast to the 6 pm required if the published[15] crystal structures of KSO_2F and $RbSO_2F$ were representative of the free SO_2F^- anion. Tables 3 and 4 also show that even the RHF calculations with a good basis set give surprisingly good results for these sulfur oxofluorides. For OSF_2, which has the same C_s symmetry as SO_2F^-, only the best coupled-cluster calculation, CCSD(T)/aug-cc-pvtz, gave a better result, i.e., a smaller average frequency deviation and smaller scaling factors, than the RHF/6-311+G(2d) calculation.

Additional evidence for the existence of a long and highly polar S−F bond in SO_2F^- comes from the structure[11] and vibrational spectra[32] of isoelectronic ClO_2F. The observed difference between the bond lengths of Cl−F and Cl=O is 27.4 pm,[11] and the structure is very similar to that predicted for free gaseous SO_2F^- (see Table 3). Further support for the geometry, predicted by us in Table 3 for free SO_2F^-, comes from a recent study of $N(CH_3)_4^+SO_2CN^-$.[33] The observed vibrational spectra were found to be in good agreement with those calculated at the RHF/6-31+G* level for a minimum-energy structure with r(S−O) = 146.7 pm, r(S−C) = 190.8 pm, $\angle$(O−S−O) = 114.0°, and $\angle$(O−S−C) = 100.8°. These structural parameters are very similar to those predicted by us for SO_2F^- in Table 3.

Normal Coordinate Analysis. The assignment and force constant of the S−F stretching mode of SO_2F^- are of significant interest. If indeed the geometry proposed in ref 15 for SO_2F^- in its K^+ and Rb^+ salts with r(S−F) = 159 pm were correct, its S−F stretching mode and force constant should be comparable to those found for SF_2 [r_e(S−F) = 159.2 pm, $\nu_{as}(SF_2)$ = 813.0 cm^{-1}, $\nu_{sym}(SF_2)$ = 838.5 cm^{-1}, f_r = 4.72 mdyn/Å].[34,35] If, on the other hand, r(S−F) in SO_2F^- falls into the range of 170−176 pm, its stretching mode and force constant should be much lower.

The assignment of the S−F stretching mode in SO_2F^- has been controversial from the very beginning. Paetzold and Aurich published the infrared and Raman spectra of KSO_2F in 1965 and assigned the 595 cm^{-1} band to the SO_2 scissoring mode and the 496 cm^{-1} band to the S−F stretching mode.[7] They attributed the surprisingly low S−F stretching frequency to a highly polar S−F bond and to fluorine bridging between the SO_2F^- ions. Shortly afterward, Seel and Boudier reported the infrared spectra of KSO_2F, $RbSO_2F$, and $CsSO_2F$. Since the frequencies of the bands at about 595 and 495 cm^{-1} changed only little for the different cations, they correctly concluded that the SO_2F^- anions should not be significantly associated. In view of the lack of significant fluorine bridging, which could have explained the low S−F stretching frequency, they proposed to assign the 595 cm^{-1} band to the S−F stretching mode.[6] In a 1990 publication on $NH_4^+SO_2F^-$, Moock and co-workers followed[9] the assignments of Paetzold and Aurich,[7] whereas in 1997 Kornath and co-workers followed[10] those of Seel and Boudier.[6] In the most recent paper,[15] Kessler and Jansen believed to have confirmed the assignments of Seel and Boudier, because they observed isolated SO_2F^- ions in the crystal structures of KSO_2F and $RbSO_2F$ and falsely assumed that Kornath's ab initio calculations had established not only the observed frequencies but also their identities. The identification of fundamental vibrations within a given symmetry species, however, requires the knowledge of the potential energy distribution (PED) obtainable through a standard normal coordinate analysis.

The results from our normal coordinate analysis of SO_2F^- are summarized in Table 5. The unscaled CCSD(T)/aug-cc-pvtz

(28) Hargittai, I.; Miglhoff, F. C. *J. Mol. Struct.* **1973**, *16*, 69.
(29) Shimanouchi, T. *J. Phys. Chem. Ref. Data* **1977**, *6*, 1021.
(30) Lide, D. R.; Mann, D. E.; Fristom, R. M. *J. Chem. Phys*. **1957**, *26*, 734.
(31) (a) Shimanouchi, T. *J. Phys. Chem. Ref. Data* **1977**, *6*, 1036. (b) Sumodi, A. J.; Pace, E. L. *Spectrochim. Acta* **1972**, *28A*, 1129. (c) Nolin, C.; Tremblay, J.; Savoie, R. *J. Raman Spectrosc*. **1974**, *2*, 71. (d) Sportouch, S.; Clark, R. J. H.; Gaufres, R. *J. Raman Spectrosc.* **1974**, *2*, 153.
(32) Smith, D. F.; Begun, G. M.; Fletcher, W. H. *Spectrochim. Acta* **1964**, *20*, 1763.
(33) Kornath, A.; Blecher, O.; Ludwig, R. *J. Am. Chem. Soc*. **1999**, *121*, 4019.
(34) (a) Kirchhoff, W. H.; Johnson, D. R.; Powell, F. X. *J. Mol. Spectrosc.* **1973**, *48*, 1157. (b) Endo, Y.; Saito, S.; Hirota, E.; Chikaraisli, T. *J. Mol. Spectrosc*. **1979**, *377*, 222.
(35) Deroche, J. C.; Buerger, H.; Schulz, P.; Willner, H. *J. Mol. Spectrosc.* **1981**, *89*, 269.

Table 3. Calculated Geometries[a] of SO_2F^- Compared to the Calculated and Observed Geometries of SOF_2 and SO_2F_2 and the Observed Geometry of ClO_2F

SOF_2						
	r_1(S−O)	$r_2 - r_1$	r_2(S−F)	∠(F−S−O)	∠(F−S−F)	ref
RHF/6−31+G*	140.9	16.7	157.6	106.6	92.5	10
RHF/6-311+G(2d)	139.5	15.9	155.4	106.5	92.6	
RHF/aug-cc-pvdz	142.6	16.6	159.2	106.3	92.3	
RHF/aug-cc-pvtz	140.1	14.7	154.8	106.3	93.0	
B3LYP/6-311+G(2d)	142.9	20.4	163.3	106.7	92.8	
B3LYP/aug-cc-pvdz	146.1	20.5	166.6	106.5	92.8	
B3LYP/aug-cc-pvtz	143.4	18.8	162.2	106.4	93.0	
CCSD(T)/6-311+G(2d)	143.1	18.8	161.9	106.7	92.3	
CCSD(T)/aug-cc-pvdz	146.9	19.3	166.2	106.4	92.3	
CCSD(T)/aug-ccpvtz	143.6	16.7	160.3	106.3	92.5	
obsd	142.0(3)	16.3	158.3(3)	106.2(2)	92.2(2)	28
SO_2F_2						
	r_1(S−O)	$r_2 - r_1$	r_2(S−F)	∠(O−S−O)	∠(F−S−F)	ref
RHF/6−311+G(2d)	138.0	12.6	150.6	124.6	95.6	
RHF/aug-cc-pvdz	141.3	13.3	154.6	125.2	94.8	
RHF/aug-cc-pvtz	138.7	11.7	150.4	124.1	95.9	
B3LYP/6-311+G(2d)	141.6	15.7	157.3	125.6	94.9	
B3LYP/aug-cc-pvdz	145.2	16.4	161.6	126.0	94.3	
B3LYP/aug-cc-pvtz	142.2	14.8	157.0	125.2	95.1	
CCSD(T)/6-311+G(2d)	141.6	14.4	156.0	125.5	94.9	
CCSD(T)/aug-cc-pvdz	145.7	15.4	161.1	126.3	94.0	
CCSD(T)/aug-cc-pvtz	142.1	13.3	155.4	125.3	95.1	
obsd	140.5	12.5	153.0	124.0	96.1	30
SO_2F^-						
	r_1(S−O)	$r_2 - r_1$	r_2(S−F)	∠(F−S−O)	∠(O−S−O)	ref
RHF/6−31+G*	145.8	24.0	169.8	100.6	113.2	10
RHF/6−31+G(3df)	143.7	22.7	166.4	100.5	112.9	14
RHF/6−311+G(2d)	144.1	19.8	163.9	100.4	113.1	
RHF/aug-cc-pvdz	147.8	23.4	171.2	100.6	112.6	
RHF/aug-cc-pvtz	144.8	21.1	165.9	100.5	112.8	
MP2/6-31+G(3df)	147.1	30.9	178.0	100.3	113.8	14
B3LYP/6-311+G(2d)	147.8	37.2	185.0	100.8	113.4	
B3LYP/aug-cc-pvdz	151.7	32.7	184.4	101.1	112.6	
B3LYP/aug-cc-pvtz	148.3	31.9	180.2	100.7	113.0	
CCSD(T)/6-311+G(2d)	147.9	34.5	182.4	100.5	113.6	
CCSD(T)/aug-cc-pvdz	152.4	30.2	182.6	100.7	112.8	
CCSD(T)/aug-cc-pvtz	148.4	27.3	175.7	100.3	115.9	
predicted	147	23−29	170−176	100.5	113	
ClO_2F						
	r_1(Cl−O)	$r_2 - r_1$	r_2(Cl−F)	∠(F−Cl−O)	∠(O−Cl−O)	ref
obsd	142.0	27.4	169.4	101.8	115.2	11

[a] Bond lengths in picometers and angles in degrees.

data were used because they duplicate the observed frequencies well and require by far the smallest scaling factors. The PED of Table 5 contains a big surprise. It shows that ν_2, ν_3, and ν_4 are all strongly mixed and that S2, the symmetry coordinate of the S−F stretch, contributes only 20% to ν_2, and 40% and 39% to ν_3 and ν_4, respectively. Thus, the S−F stretch is distributed over all three fundamental vibrations and is concentrated in ν_3 and ν_4. An inspection of the signs in the PED reveals the following coupling effects: (580 cm^{-1}) in-phase coupling of $\delta_{sym}(FSO_2)$ (45%) with $\delta_{sciss}(SO_2)$ (31%) and their out-of-phase coupling with ν(SF) (20%); (506 cm^{-1}) in-phase coupling of $\delta_{sciss}(SO_2)$ (56%) with ν(SF) (40%) and their out-of-phase coupling with $\delta_{sym}(FSO_2)$ (3%); (365 cm^{-1}) in-phase coupling of $\delta_{sym}(FSO_2)$ (51%) with ν(SF) (39%) and their out-of-phase coupling with $\delta_{sciss}(SO_2)$ (10%). This analysis demonstrates the irrelevance and fallacies of arguments over the assignment of certain modes without the benefits of a normal coordinate analysis. As is often the case, nature disregards our desire to paint simple black and white pictures of complex issues.

A second surprising result from the normal coordinate analysis is the very small value of 1.6 mdyn/Å for the S−F stretching force constant. Normal, predominantly covalent S−F bonds exhibit values ranging from about 4.5 to 5.4 mdyn/Å.[36,37] The low value of the S−F stretching force constant demonstrates the high polarity of the S−F bond in SO_2F^-. Furthermore, the 39% contribution of S−F stretching to the low-frequency 365 cm^{-1} mode provides a dissociative pathway with a low activation energy barrier toward the loss of a fluoride ion.

Conclusions

(i) The experimental crystal structures of the TMA^+, TAS^+, $TAOS^+$, and K^+ salts of SO_2F^- show that all the crystal structures reported so far for SO_2F^- suffer from severe oxygen/

(36) Haas, A.; Willner, H. *Spectrochim. Acta* **1979**, *35A*, 953.
(37) Siebert, H. *Anwendungen der Schwingungsspektroskopie in der Anorganischen Chemie; Anorganische und Allgemeine Chemie in Einzeldarstellungen, VII*; Springer-Verlag: Berlin, 1966.

Table 4. Calculated Scaled (Unscaled) and Observed Vibrational Frequencies of SO_2F_2, SOF_2, and SO_2F^-

SO_2F_2 (C_{2v})

	a_1				a_2	b_1		b_2		av	
	ν_1	ν_2	ν_3	ν_4	ν_5	ν_6	ν_7	ν_8	ν_9	$\Delta(\nu_{obsd} - \nu_{calcd})$	ref
obsd	1270	849	553	384	384	1504	544	887	540		31
RHF/6-311+G(2d)	1259(1384)	869(955)	557(612)	384(422)	379(417)	1473(1619)	547(595)	897(986)	541(601)	9.4	
RHF/aug-cc-pvdz	1234(1305)	881(932)	561(569)	383(389)	374(380)	1444(1528)	555(551)	913(966)	543(563)	21.5	
RHF/aug-cc-pvtz	1246(1393)	876(979)	550(615)	385(426)	380(421)	1453(1624)	558(601)	904(1010)	542(606)	15.9	
IR and RA int[a]	212.5,13.0,0.09	128.2,11.5,0	47.9,1.7,0.73	0.12,0.64,0.75	0,0.99	384.3,1.72	44.7,1.21	276.5,1.81	42.1,1.29		
B3LYP/6-311+G(2d)	1304(1226)	823(774)	557(516)	383(355)	383(355)	1553(1460)	546(506)	859(808)	542(502)	16.3	
B3LYP/aug-cc-pvdz	1281(1162)	841(763)	560(477)	380(324)	378(322)	1518(1377)	551(466)	875(794)	547(469)	8.4	
B3LYP/aug-cc-pvtz	1287(1231)	837(800)	557(520)	384(359)	383(358)	1527(1460)	547(511)	870(832)	541(505)	7.5	
CCSD(T)/6-311+G(2d)	1289(1238)	833(800)	555(532)	387(372)	382(366)	1531(1471)	544(521)	876(841)	538(515)	9.0	
CCSD(T)/aug-cc-pvdz	1262(1159)	848(779)	558(484)	385(334)	377(327)	1498(1376)	548(474)	893(820)	546(475)	4.9	

SOF_2 (C_s)

	a′				a″			
	ν_1	ν_2	ν_3	ν_4	ν_5	ν_6	$\Delta(\nu_{obsd} - \nu_{calcd})$	ref
obsd	1333	808	530	378	747	393		29
RHF/6-311+G(2d)	1321(1457)	811(894)	533(601)	380(428)	751(828)	389(439)	4.7	
RHF/aug-cc-pvdz	1269(1389)	822(900)	536(565)	376(396)	773(846)	391(412)	19	
RHF/aug-cc-pvtz	1288(1466)	819(932)	531(611)	377(434)	764(870)	390(449)	11	
B3LYP/6-311+G(2d)	1420(1313)	794(734)	535(486)	369(335)	716(662)	399(362)	25	
B3LYP/aug-cc-pvdz	1348(1261)	804(752)	540(465)	364(313)	743(695)	401(345)	5.0	
B3LYP/aug-cc-pvtz	1370(1318)	802(771)	535(501)	370(346)	733(705)	398(373)	12	
CCSD(T)/6-311+G(2d)	1390(1307)	798(750)	532(500)	376(354)	729(685)	392(369)	12.7	
CCSD(T)/aug-cc-pvdz	1313(1241)	809(765)	536(469)	369(324)	757(716)	399(349)	8.7	
CCSD(T)/aug-cc-pvtz	1330(1322)	808(803)	531(517)	378(368)	749(745)	392(381)	1.2	

SO_2F^- (C_s)

	a′				a″			
	ν_1	ν_2	ν_3	ν_4	ν_5	ν_6	$\Delta(\nu_{obsd} - \nu_{calcd})$	ref
obsd	1108	590	497	387	1184	363		10
RHF/6-31+G*	1086	605	536	394	1174	362	15.7	10
RHF/6-311+G(2d)	1098(1219)	597(663)	511(567)	377(418)	1184(1314)	362(402)	6.8	
RHF/aug-cc-pvdz	1088(1163)	611(653)	529(584)	381(421)	1166(1247)	347(383)	18.8	
RHF/aug-cc-pvtz	1088(1227)	608(686)	514(612)	384(458)	1170(1319)	354(422)	13.5	
B3LYP/6-311+G(2d)	1114(1079)	571(553)	554(472)	364(310)	1218(1179)	350(298)	25.3	
B3LYP/aug-cc-pvdz	1117(1034)	578(535)	558(479)	371(318)	1200(1111)	340(292)	22.8	
B3LYP/aug-cc-pvtz	1113(1086)	577(563)	540(490)	370(336)	1206(1177)	351(318)	18.7	
CCSD(T)/6-311+G(2d)	1105(1076)	576(561)	538(475)	367(324)	1215(1183)	355(313)	19.5	
CCSD(T)/aug-cc-pvdz	1102(1017)	589(543)	550(485)	364(330)	1193(1101)	342(302)	17.2	
CCSD(T)/aug-cc-pvtz	1102(1092)	585(580)	525(506)	378(365)	1201(1190)	352(340)	12.7	

[a] IR and Raman intensities in km mol^{-1} and $Å^4$ amu^{-1}, respectively, and polarization ratios.

Table 5. Unscaled CCSD(T)/aug-cc-pvtz Symmetry Force Constants and Potential Energy Distribution of SO_2F^- [a]

calcd freq (cm^{-1})				symmetry force constants[b]				PED[c]			
				F_{11}	F_{12}	F_{33}	F_{44}				
a′	ν_1	1092	F_{11}	8.520				96.6(1)	2.9(3)	0.6(4)	
	ν_2	580	F_{22}	0.486	1.626			45.0(4)	31.3(3)	20.4(2)	3.4(1)
	ν_3	506	F_{33}	0.220	−0.076	1.913		56.1(3)	40.4(2)	3.4(4)	
	ν_4	365	F_{44}	−0.007	0.014	0.596	1.924	50.9(4)	39.3(2)	9.8(3)	
				F_{55}	F_{66}						
a″	ν_5	1190	F_{55}	7.840				99.1(5)	0.8(6)		
	ν_6	340	F_{66}	0.100	1.049			99.1(6)	0.8(5)		

[a] $f_{iso} = 8.180$, $f_{SF} = 1.626$. [b] Stretching force constants in mdyn/Å, deformation constants in (mdyn Å)/rad^2, and stretch−bend interaction constants in mdyn/rad. [c] PED in percent; the symmetry coordinates are defined as (1) $\nu_{sym}(SO_2)$, (2) $\nu(SF)$, (3) $\delta_{sciss}(SO_2)$, (4) (3) $\delta_{sym}(O_2SF)$, (5) $\nu_{asym}(SO_2)$, and (6) $\delta_{asym}(O_2SF)$.

fluorine disorder and that the given geometries do not reflect the true structure of SO_2F^-. In the structures of the TMA^+, TAS^+, and $TAOS^+$ salts, one oxygen atom is ordered and its S−O distance of 147 pm is well defined. The S−F distances can be estimated to equal or exceed 170 pm by refining the occupancy factors in the O/F disorders and by an extrapolation of a correlation between the occupancy factors and the observed bond lengths to 100% occupancy.

(ii) Theoretical calculations and a comparison with isoelectronic ClO_2F, which does not suffer from disorder problems, were used to predict the ideal structure of free SO_2F^-. The predicted structure agrees well with the crystallographic results.

(iii) The good agreement between observed and calculated vibrational frequencies lends additional support to the theoretically predicted geometry of SO_2F^-. The previous conclusion[15] that the observed frequencies were and can be duplicated computationally with a grossly incorrect geometry is untenable.

(iv) A normal coordinate analysis of SO_2F^- shows that the S−F stretching and the two deformation motions in the a′ block are strongly coupled. In contrast to all previously proposed assignments, the S−F stretch is concentrated in the two lowest frequency modes, resulting in a surprisingly low S−F stretching force constant of 1.63 mdyn/Å and a low energy barrier toward F^- loss. The low value of the S−F stretching force constant provides further support for the presence of an unusually long S−F bond in SO_2F^-.

(v) The previous controversy between experimental and theoretical results for SO_2F^- has been resolved in favor of the theoretical predictions.

Acknowledgment. The work at the University of Bremen was financially supported by the Deutsche Forschungsgemeinschaft, that at USC by the National Science Foundation, and that at the Air Force Research Laboratory by the Air Force Office of Scientific Research. This work was also supported in part by a grant of Cray T916 time from the Army Research Laboratory Department of Defense, High Performance Computing Center.

Supporting Information Available: Tables of structure determination summaries, atomic coordinates, bond lengths and angles, anisotropic displacement parameters, and hydrogen coordinates of **1**−**4**. This material is available free of charge via the Internet at http://pubs.acs.org.

IC000616P